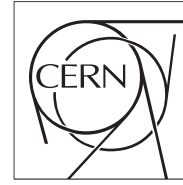




The Compact Muon Solenoid Experiment
Conference Report

Mailing address: CMS CERN, CH-1211 GENEVA 23, Switzerland



02 November 2015 (v2, 06 November 2015)

Low-Cost Bump-Bonding Processes for High Energy Physics Pixel Detectors

M. Caselle*, T. Blank, F. Colombo, A. Dierlamm, U. Husemann, S. Kudella, M. Weber for the CMS Collaboration

Abstract

In the next generation of collider experiments detectors will be challenged by unprecedented particle fluxes. Thus large detector arrays of highly pixelated detectors with minimal dead area at reasonable costs are required. Bump-bonding of pixel detectors has been shown to be a major cost-driver. KIT is one of the production centers of the CMS barrel pixel detector for the Phase I Upgrade. In this contribution the SnPb bump-bonding process and the production yield is reported. In parallel to the production of the new CMS pixel detector, several alternatives to the expensive photolithography electroplating/electroless metal deposition technologies are developing. Recent progress and challenges faced in the development of bump-bonding technology based on gold-stud bonding by thin ($15\ \mu\text{m}$) gold wire is presented. This technique allows producing metal bumps with diameters down to $30\ \mu\text{m}$ without using photolithography processes, which are typically required to provide suitable under bump metallization. The short setup time for the bumping process makes gold-stud bump-bonding highly attractive (and affordable) for the flip-chipping of single prototype ICs which is the main limitation of the current photolithography processes.

Presented at *TWEPP 2015 TWEPP 2015 - Topical Workshop on Electronics for Particle Physics*

Low-Cost Bump-Bonding Processes for High Energy Physics Pixel Detectors

M. Caselle^{*a}, T. Blank^a, F. Colombo^b, A. Dierlamm^{ab}, U. Husemann^b, S. Kudella^b and M. Weber^{ab} for the CMS Collaboration

^a*Institute for Data Processing and Electronics (IPE), Karlsruhe Institute of Technology (KIT)
Hermann-von-Helmholtz-Platz 1, 76344 Eggenstein-Leopoldshafen, Germany*

^b*Institut für Experimentelle Kernphysik (IEKP), Karlsruhe Institute of Technology (KIT)
Wolfgang-Gaede-Str. 1, 76131 Karlsruhe, Germany*

E-mail: michele.caselle@cern.ch

ABSTRACT: In the next generation of collider experiments detectors will be challenged by unprecedented particle fluxes. Thus large detector arrays of highly pixelated detectors with minimal dead area at reasonable costs are required. Bump-bonding of pixel detectors has been shown to be a major cost-driver. KIT is one of the production centers of the CMS barrel pixel detector for the Phase I Upgrade. In this contribution the SnPb bump-bonding process and the production yield is reported. In parallel to the production of the new CMS pixel detector, several alternatives to the expensive photolithography electroplating/electroless metal deposition technologies are developing. Recent progress and challenges faced in the development of bump-bonding technology based on gold-stud bonding by thin ($15\ \mu\text{m}$) gold wire is presented. This technique allows producing metal bumps with diameters down to $30\ \mu\text{m}$ without using photolithography processes, which are typically required to provide suitable under bump metallization. The short setup time for the bumping process makes gold-stud bump-bonding highly attractive (and affordable) for the flip-chipping of single prototype ICs which is the main limitation of the current photolithography processes.

KEYWORDS: Bump-Bonding; Gold-Stud Bumping; Pixel Detector; LHC Upgrade.

Contents

1. Introduction	1
2. Bare module production for the CMS Phase I Upgrade pixel detector	1
2.1 Eutectic-SnPb bumping process and UBM deposition	2
2.2 Pre-bonding process	3
2.3 Bonding process	3
2.4 Bare module test and reflow process	4
2.5 Process yield and reworking	5
3. Emerging bump-bonding technology based on gold-stud bumping	6
4. Comparison between bump-bonding technologies	7
5. Conclusions	8

1. Introduction

For the Phase I Upgrade (2016/17), the CMS pixel detector needs to be replaced [1]. The new barrel pixel detector consists of four concentric layers. Compared to the present CMS pixel barrel, there is one additional layer at high radius. The new barrel will be populated with the total of 1184 rectangular modules, with a total number of pixels increased by a factor 1.6 from 48 M to 79 M pixels. Due to the large number of required modules the production has been distributed to several institutions/countries. Layer one and two are being produced by a Swiss consortium (PSI, ETH Zürich, University of Zürich), the third layer is produced by Italy/CERN/Taiwan/Finland and the fourth layer by the German consortium (DESY, University of Hamburg, KIT, RWTH Aachen). The pixel bare module consists of a sensor with a matrix of 66560 pixels bump-bonded to 16 readout chips, PSI46dig [2]. Each readout chip contains 4160 pixels arranged in a matrix of 52×80 elements with a pixel size of $150 \times 100 \mu\text{m}^2$. KIT has the responsibility of producing 21% of the modules plus 20% of the spare modules. The total production volume is approximately 350 bare modules with more than 6000 known-good-dice to be bonded.

2. Bare module production for the CMS Phase I Upgrade pixel detector

The bump-bonding process tends to dominate the costs and production schedule of pixel detectors. To reduce the production costs and to optimize the production schedule, KIT has decided to buy the bumping process in industry and to perform the bonding process (flip-chip) in-house. The bump deposition on the ROC (ReadOut Chip) wafer is performed by RTI [3]. It consists of $30 \mu\text{m}$ SnPb

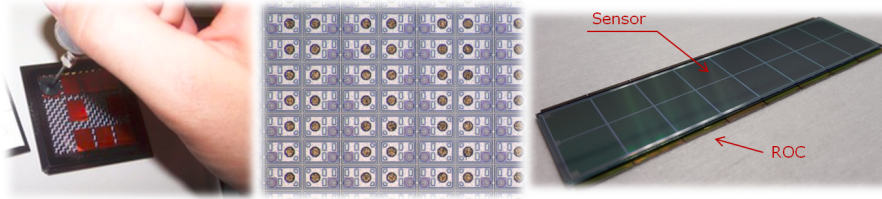


Figure 1. Bumped ROCs die from RTI covered by protective photoresist (left). UBM metal deposition on the sensor die (center). CMS pixel detector bare module produced at KIT (right).

bumps electroplated onto a standard Ni-Au under-bump-metallization (UBM). After the bumping, the ROC wafers are thinned to $175\ \mu\text{m}$, diced, optically inspected and then sent for the flip-chip process. The sensor wafers require a UBM metal deposition. In order to reduce costs and risks, the UBM technology has been shared with DESY allowing the exchange of sensors between institutes. PacTech [4] has been selected for the UBM process. KIT receives both the bumped ROCs and the processed sensors and performs the bonding using a Fineplacer-Femto bonder machine [5]. Figure 1 shows the bumped ROCs, the UBM deposition on the sensor and a bare module produced. The following sections describe the process steps developed for the bare module production.

2.1 Eutectic-SnPb bumping process and UBM deposition

Bumping is an advanced wafer level process technology where “bumps” or “balls” made of solder are formed at the wafer level before the wafer is diced into individual chips. Those “bumps”, which can be composed of eutectic, lead-free, high-lead materials or Cu-pillars, are the fundamental interconnect components that will connect the readout chip and the sensor. These bumps not only provide a connection between readout chip and sensor, but also play an important role in the electrical, mechanical and thermal performance; therefore they must exhibit superior adhesion to the die, minimal ohmic electrical resistance, and result in high assembly yields. During the R&D phase, several bumping vendors have been investigated and several bumping processes have been characterized. Two bumping processes by RTI have been investigated. The first is based on eutectic-SnPb bumps while the second on Cu-pillar bumps. The Cu-pillar bumps are typically formed in a process similar to electroplated solder bumps; a thick layer of Cu is plated prior to the solder and later reflowed to form a rounded solder cap on top of the Cu. Figure 2 shows a cross-section of the assemblies with a single ROC bonded by the Fineplacer-Femto bonder machine. For both bumping technologies UBM metal deposition is necessary on the sensor die only. The bonding pad opening size in the ROC is only $15\ \mu\text{m}$ and therefore an enlarged passivation opening is necessary prior to the UBM metal deposition to accommodate the $30\ \mu\text{m}$ bump [3]. The enlarged passivation opening is visible in Figure 2 (left). Contrary to SnPb bumps in Cu-pillar technology the pillar is deposited directly onto the ROC wafer, as can be seen in Figure 2 (right). This results in fewer photolithographic steps and lower production costs. Excellent mechanical and electrical performance has been achieved by both bumping technologies. In order to keep a better uniformity of bumping technologies within the collaboration, KIT has decided to use the standard SnPb solder bumping process for series production. After the bumping, the ROCs are thinned, diced and covered with a thick photoresist layer by RTI to protect against handling damage, particulate contamination and bump oxidation. The sensor bump openings are covered by a ENEPIG (Electroless Ni, Electroless

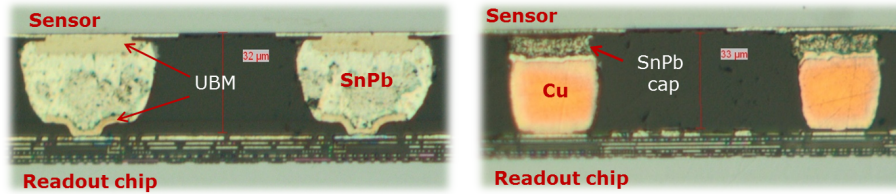


Figure 2. Cross-section of the bonding assembly using different bumping technologies, based on eutectic-SnPb (left) and Cu-pillar technology (right). In both cases, the sensor substrate is located at the top and the readout chip at the bottom with a separation between dice of about 32 – 33 μm .

Pd and Immersion Gold) UBM by PacTech [4]. After the UBM deposition, the sensors are diced and optically inspected. KIT receives the bumped ROCs delivered in a Gel-Pack™ from RTI and the sensor die with UBM deposition from PacTech and performs the flip-chip process.

2.2 Pre-bonding process

Before the bonding process, the protecting thick photoresist needs to be removed by a cleaning procedure. The ROCs are placed on a custom-designed tray made of ESD-safe Polyoxymethylene (POM). The ROCs positioned on the tray are cleaned with a sequence of three different solvent baths. The first bath consists of ultrapure (> 99%) acetone which quickly dissolves the photoresist layer and other possible organic contaminants. Since acetone is a non-polar compound and it is not possible to mix it with water, an intermediate bath with ultrapure isopropyl alcohol is needed for washing away the residual acetone. The cleaning process is completed by a sequence of two baths in distilled and filtered water. While optimizing the cleaning procedure, the quality of the results was checked by inspecting a cleaned chip under a scanning electron microscope. During the production workflow, the cleaned ROCs and the sensor die are optically inspected by an automated digital microscope. The high-resolution digital pictures of each component are fed to custom-made pattern recognition software which automatically searches for the defective bumps or contaminations. After cleaning and optical inspection, the ROCs are transferred to the Gel-Pack, with the bumped area facing down, therefore arranged in a regular pattern, ready for being picked up by the bonding machine. All sensors are electrically tested by a dedicated probe station in order to check the quality of the sensor die after the UBM deposition and dicing process.

2.3 Bonding process

To guarantee high quality of the bonding process, a high-quality control of the cleaning process is required. Only the sensors and the cleaned ROCs that satisfy the optical inspection criteria will be bonded to form the bare modules. Figure 3 (left) shows the clean room (class 1000) for the bonding process, and the internal organization. The clean room is equipped with the Fineplacer-Femto automated flip-chip machine, the dedicated reflow oven and the made-in-house automated probe station for the bare module test. The sensor die is placed on the bonding table by the operator, and the position of the sensor is precisely measured and aligned. This is done automatically using alignment marks on the sensor and a pattern recognition algorithm. Then a first ROC placed face down on a Gel-Pack is picked by the pick-and-place-tool and held by vacuum. Its position is also precisely measured with the internal microscope. The ROC undergoes an electrical functionality

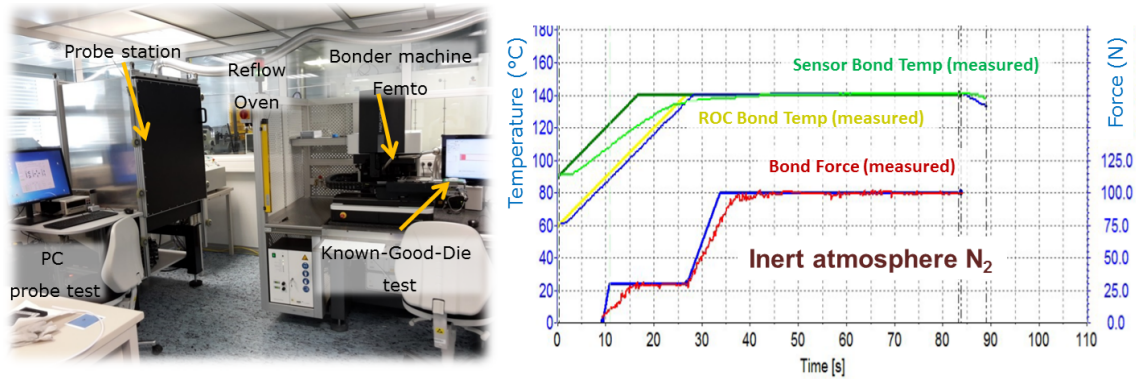


Figure 3. Overview of the clean room (class 1000) for the bonding process (left) and the bonding diagram (right).

test (known-good-die) using the probe card directly mounted on the bonding machine as shown in Figure 3. Only working ROCs are bonded to the sensor. After the electrical test the bonding is performed with the bonding parameters shown in Figure 3 (right). The bond force and temperature were deeply investigated in order to maximize the metal (SnPb on ROC) to metal (UBM on sensor) connection already prior to the reflow process. The higher metal-to-metal connection results in a high mechanical strength and excellent quality of the electrical connection. A bond temperature above 120 °C is necessary to enable a large diffusion area of SnPb bumps onto the UBM deposition. To guarantee a good homogeneous diffusion the bond temperature profile is set to 140 °C for both sensor and ROCs. By selecting the same temperature for both substrates additional stress due to the mismatch of the thermal conditions is avoided. The bond force is responsible to connect the bump and UBM with a strong mechanical contact during the bonding process. The bond force defines the bump deformation and the gap separation between the sensor and ROCs. During the bonding process two bond force steps are present. The first works as an initial touch-down force and then the process bond force of 100N (about 24mN per bump) is applied for a bond time of 50 seconds with stable temperature. The bonding is performed in an inert atmosphere. This procedure is repeated for all 16 readout chips. The placement of 16 ROCs on a sensor takes about 50min including the chip test plus about 15 min for loading the machine and preparing the components. During the ROC bonding no human intervention is necessary. This allows a throughput of several bare modules per day, sufficient for the production of some hundreds of modules within a few months.

2.4 Bare module test and reflow process

After the bonding process, the bare module is tested on the probe station shown in Figure 3. The test includes different stages. The easiest method for testing sensors is to take a current-voltage characteristic (IV-curve), since already small damage leads to an increase of the leakage current, if the damage is inside the space charge region. The ratio between the leakage current measured with a voltage set on the sensor of 250 V and 150 V is also considered in the final sensor grade. After the sensor test, each ROC is individually tested to check the correct behavior of the circuits and the number of defective pixels. We distinguish between dead and noisy pixels and missing

bump-bonding connections. According to the test results, the bare modules are divided into three grades, A, B and C: (A) IV-curve with a leakage current $I < 2 \mu\text{A}$ @ 150 V with a ratio < 2 and less than 1% defective pixels per ROC; (B) IV-curve with $2 \mu\text{A} < I < 10 \mu\text{A}$ @ 150 V and a ratio < 2 and less than 4% defective pixels; (C) IV-curve $I > 10 \mu\text{A}$ or large ratio or more than 4% of defective pixels for one or more ROCs. If the bare module is grade A, the assembly undergoes a reflow process performed in a dedicated oven. Otherwise the bare modules will be reworked (Section 2.5). Up to 6 bare modules can be reflowed simultaneously. The reflow process is performed under vacuum until the peak temperature is achieved. The peak temperature has been set to a value sufficiently higher than the melting point of the eutectic-SnPb to enable a perfect wetting of the solder bumps on the UBM. The peak temperature of the reflow is set to 240°C and is held for 30 seconds. In addition the surface tension of the SnPb provides a self-alignment mechanism between sensor and ROCs. During the cooling phase formic acid is applied when the bumps are still in the liquid phase which improves the final bump shape. Figure 2 (left) shows a cross-section of the bump-bonded structure. Both UBM layers are fully wetted by SnPb without any void inside the bumps. Sensor and ROCs are well aligned thanks to the self-alignment mechanism during the reflow. Moreover, inter-metallic formation is negligible resulting in high mechanical strength. The formation of micro-voids inside the bumps have been deeply investigated during the R&D phase using high-definition micro X-ray radiography [6].

2.5 Process yield and reworking

In this section the preliminary production yield of the first 80 bare modules produced, about 31 % of the total production, will be reported and the quality of the process discussed. Figure 4 (left) shows the current production yield calculated for the total number of bare modules produced. According to the bare module grading described in Section 2.4, 92 % of the bare modules produced are grade (A) while 6 % are grade (B). Only a small fraction of the bare modules are not accepted for module production (grade C). In particular, considering the total number of ROCs bonded (more then 800), 85% show no defective pixels, 10 % show less than six defective pixels and only 5 % of the ROCs show more than six defective pixels. The leakage current distributions measured before and after the flip-chip process is reported in Figure 4 (right). An average leakage current of $0.9 \mu\text{A}$ at a bias voltage of 150 V is measured and compared with the mean value before the bonding. The small variation between the distributions indicates that the residual mechanical stress induced due to the

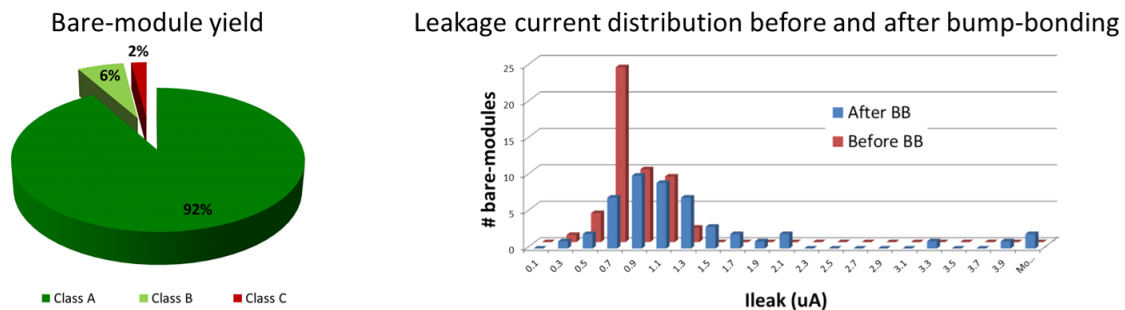


Figure 4. Bump-bonding production yield (left) and leakage current distributions @ 150V (room temperature) before and after the bump-bonding (BB) (right).

bonding process is very small.

A major benefit of an in-house bonding process is the possibility of establishing a practical rework process. A low-temperature rework procedure has been successfully developed and used instead of a high-temperature process that would require a liquid phase of the SnPb bumps during the die separation. The rework is performed before the reflow and after the bare module test so that the initial diffusion due to the bonding is strong enough for handling/testing the bare module and soft enough for the separation of a single ROC from the sensor by the pull-test on the bonder machine.

3. Emerging bump-bonding technology based on gold-stud bumping

Gold-stud bump-bonding is a modification of the mature standard ball-to-wedge gold wire bonding process. Like in wire bonding, the ball is bonded to the die pad. Then the wire is terminated after the first bond, so there is only a gold bump deposited on the die pad. The gold-stud bumping process is mainly performed at the wafer level for volume production applications. The possibility to perform the bumping process on single die is very attractive. With gold-stud bumping, contrary to other wafer bumping processes such as solder deposition, the wafer does not require pre-treatment such as UBM deposition or redistribution layers (RDL). This provides cost savings and a short process setup-up time due to the direct gold bump deposition on the top aluminum metal layer of the bond pads. Figure 5 (right) shows the gold-stud bumping process on a dummy daisy-chain MAPSA (MACRO Pixel Sub Assembly) wafer for the pixel-strip (PS) module of the CMS outer tracker for HL-LHC [7]. The daisy-chains are used to check and measure bump resistance. The bumping process is performed by a Kulicke & Soffa® - IConn ball-wedge bonder machine with the special AccuBump process profile [8]. In Figure 5 (left) the main components of the bond head are visible: the wire clamp, the capillary and the Electric Flame-Off (EFO). The process can be divided into four steps: High voltage is applied by EFO close to the tip of the gold wire causing a spark that melts the gold wire into a Free Air Ball (FAB). Then, the capillary goes into contact with the substrate and starts the thermosonic bonding. The bond force, ultrasonic power, time and temperature need to be optimized for a reliable metal-to-metal connection. Finally, the wire gets

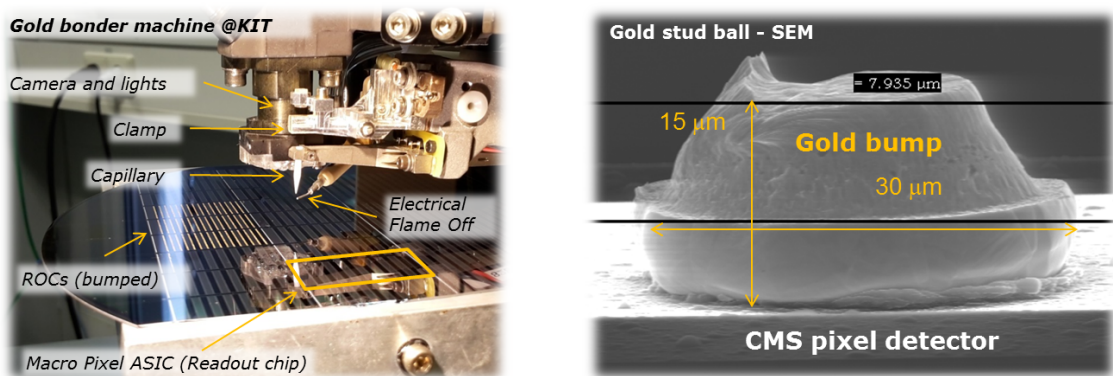


Figure 5. Ball-wedge bonder and wafer bumping process of a dummy daisy-chain wafer of a Macro Pixel ASIC (MPA) for Pixel-Strip modules of the CMS Phase II Upgrade (left). Scanning Electron Microscopy picture of a $30\ \mu\text{m}$ gold-stud bump placed on a pixel detector using a $15\ \mu\text{m}$ wire (right).

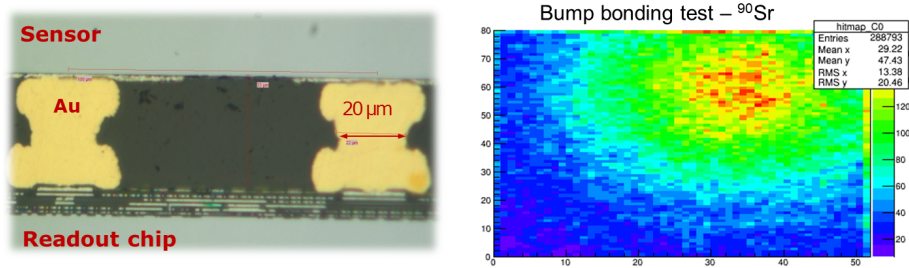


Figure 6. Cross-section of a bump-bonding assembly using the gold-stud bump-bonding technology (left) and an electrical test with a ^{90}Sr source.

sheared above the gold-stud bump, creating a smooth bump height and an initial breaking point for re-feeding the wire for the next FAB. The bump diameter and the minimum pitch between bumps are defined by the gold wire diameter, the capillary used and the machine settings. Figure 5 (right) shows a scanning electron microscope picture of a gold-stud deposited on a CMS pixel sensor using a gold wire with a diameter of $15\ \mu\text{m}$. A bump diameter of only $30\ \mu\text{m}$ and a bump height of $15\ \mu\text{m}$ has been achieved. Moreover, the bump shape is comparable with the bump deposited by standard photolithography processes. The bonder machine is capable of placing up to 20 bumps/s with a very high bump reproducibility. The low non-recurring engineering (NRE) production costs and fast process setup time are the major benefits of this technology that could be employed during the IC prototyping phase. After the gold-stud bumping deposition the flip-chip bonding is performed by a thermo-compression bonding process. A very strong mechanical connection and excellent electrical performance are achieved with a temperature range between 200 and 300 °C and bond forces from 48 to 80 mN/bump according to the gold-stud bump size. Figure 6 (left) shows a cross section after the bonding. A very clean metal-to-metal interface without any voids is visible. The electrical performance of the assembly was tested using a ^{90}Sr -source. The assembly was fully functional, no bump was missing.

4. Comparison between bump-bonding technologies

In this section a preliminary comparison between different bump-bonding technologies available is reported. In particular we compare the process parameters for SnPb, Cu-pillar and gold-stud bumping using a single ROC bonded on a single sensor as a test vehicle. Table 1 shows the bonding parameters used for each bumping technology and the reflow peak temperature. Like the SnPb bumping technology, the Cu-pillar bumps establish the metal connection by a small SnPb cap, therefore the temperatures of both the bonding and reflow processes are in the same range. For Cu-pillar bumps, only a small amount of SnPb metal needs to be deformed while the Cu-pillar preserves the same shape, so that a reduced bond force is sufficient to establish a metal connection comparable to SnPb bumps. The bonding process for gold-stud bumps requires higher bond temperature and force compared to the solder bumps. Contrary to the previous technologies, no bump reflow process is necessary so that the total process time is limited by the bonding phase of 50 seconds while the total process time for SnPb and Cu-pillar bumps is dominated by the reflow process of approximately ten minutes. The mean value of the mechanical strength measured by a

Table 1. Comparison between different bump-bonding technologies available at KIT.

Bumping tech.	Bond force/bump	Bond temp.	Reflow (peak temp.)	Pull test (4160 bumps)
Eutectic-SnPb	24 mN	130 °C	240 °C	9 kg
Cu-pillar	19 mN	130 °C	240 °C	7 kg
Au stud ball	48 mN	250 °C	No Reflow	> 10 kg

destructive pull-test is also reported in Table 1. All processes exhibit a high mechanical strength of more than 1.6 g/bump. The gold-stud technology shows a higher mechanical strength which exceeds the maximum force of the pull-test machine. A systematical measurement of the bump yield is carried out by measurements with particles and X-rays. For a correct comparison of the noise and efficiency between the different technologies, ROC and sensor have been carefully kept at the same separation gap for all assemblies, so that the parasitic capacitance of the bump-bonding was comparable between the different technologies. All technologies show a bump yield close to 100% with the noise within the normal range.

5. Conclusions

In this contribution an overview of the bump-bonding process for the production of the CMS pixel detector for the Phase I Upgrade has been presented. So far, based on 80 bare modules, a high production yield of 92 % has been achieved at a production rate of four bare modules/day. In parallel, a very low-cost bump-bonding process based on gold-stud bumping suitable for single prototype IC and wafer level has been developed. This technique allows producing metal bumps with high-density pitch without using photolithography processes. The process exhibits excellent mechanical and electrical properties. Further tests are planned in order to check the gold activation in the HL-LHC radiation environment. Preliminary results exhibit that the gold bumping technology can be used for the next generation of pixel detectors. Currently, the gold-stud bump-bonding technology has been tested for the flip-chip of Pixel-Strip (PS) modules of the CMS Phase II Upgrade.

References

- [1] CMS Collaboration, *CMS Technical Design Report for the Pixel Detector Upgrade*, CERN-LHCC-2012-016, **CMS-TDR-011** (2012).
- [2] J.A. Gray, *The CMS Phase-1 pixel detector*, 2013 *JINST* **8** C12047.
- [3] A. Huffman, et al., *Fine-Pitch Wafer Bumping and Assembly for High Density Detector Systems*, *Nuclear Science Symposium Conference Record*, October, 19-25, 2003. Vol. 5, pp 3522-3526.
- [4] PacTech - Packaging Technologies GmbH, *Electroless Nickel Plating*, <http://www.pactech.com> (2015).
- [5] Finetech, *FINEPLACER femto*, <http://eu.finetech.de> (2015).
- [6] T. Blank, M. Caselle, et al., *Novel module production methods for the CMS pixel detector upgrade phase I*, 2015 *JINST* **10** C02021.
- [7] D. Ceresa, et al., *Macro Pixel ASIC (MPA): the readout ASIC for the pixel-strip (PS) module of the CMS outer tracker at HL-LHC*, 2014 *JINST* **9** C11012.
- [8] Kulicke & Soffa, *Process Users Guide AccuBump Process Profile*, March 14, 2005 Rev. 1.7.